Using AUV-Acquired Survey Data to Derive a Magnetic Model for a Surface Vessel

David Schipf[1], John Feusi[1], Michael Anderson[1], Eric Wolbrecht[1], John Canning[1], Dean Edwards[2]
[1]Department of Mechanical Engineering, University of Idaho, Moscow, Idaho
[2]Department of Chemical Engineering, University of Idaho, Moscow, Idaho

***Abstract*— To develop an inverse model of the magnetic signature of a surface vessel, autonomous underwater vehicles (AUVs) equipped with tri-axial, flux-gate magnetometers were used to acquire magnetic field measurements underneath the moving surface vessel. Measurements were taken by AUVs operating in a formation at 3-7 m depth below the water surface. Multiple magnetic dipoles were used to model and estimate the magnetic signature of the surface vessel from the measurements. AUV orientation was estimated from onboard inertial measurement unit (IMU) and magnetic compass measurements in an attempt to transform the measured magnetic field vector components into the Earth's inertial frame. An uncertainty propagation study predicted ~18 nT root-mean-squared (RMS) noise in the magnetic field vector components resulting from uncertainty in AUV orientation estimation and uncertainty in the magnetometer measurements. The impact of network latency in the AUV distributed control system on the magnetic field vector components was discussed. A measured deviation in the transformed, inertial frame magnetic field vertical component of ~220 nT was compared with predicted values.**

Keywords—AUV; magnetic signature; dipole inversion; orientation estimation

I. INTRODUCTION

Detonation of underwater mines can be triggered by the magnetic signature of a surface vessel altering the background magnetic field. Magnetic fields in the extremely low frequency (ELF) range of 3 Hz to 3kHz and the ultra low frequency (ULF) range from ~0 to 3Hz [1] are subject to underwater mine detection. Active cancellation of the magnetic signature can be accomplished, but estimation of the magnetostatic field associated with the vessel is needed.

A surface vessel with a ferromagnetic hull generally contains a remnant magnetic field that depends on the magnetic history of the hull [2]. The remnant magnetic field can be estimated by forward or inverse modeling. Forward models are analytically based, while Inverse models rely on experimental data [3]. Measurements for inverse models can be collected from full size surface vessels in static test facilities or from physically scaled models with fixed magnetic sensors [2] [4].

It is advantageous to use in-situ measurements of the magnetic field for estimating the magnetic signature of a surface vessel rather than taking measurements while the vessel is at a static test facility. Once the surface vessel leaves the static test facility, the magnetic signature of the vessel is subject to change. This change can be predicted by forward models, but the signature estimation of a ship is complex and difficult to estimate with simulation [3]. A simpler approach could be to take additional measurements after the magnetic field has changed.

Autonomous underwater vehicles (AUVs) equipped with magnetometers could theoretically acquire measurements of the magnetic signature of a moving surface vessel after the vessel has been deployed [5] [6]. This requires accurately measured relative position from the surface vessel to the magnetic field sensors onboard the AUVs. If vector magnetic field measurements near the surface vessel are used, the orientation of the magnetometer is needed to determine the field in the Earth's inertial frame. AUV-acquired measurements of a vector magnetic field thus require the simultaneous position and orientation measurements of the rigidly mounted magnetometer.

The use of AUVs to acquire magnetic field measurements presents challenges. Magnetic noise can come from onboard materials and electronics during AUV movements [7]. Total field–or the magnitude of the magnetic field–measurements have been used to derive magnetic signature models [5] [6]. The use of the magnitude of the magnetic field measurements instead of vector field components constrains inverse modeling approaches and provides 1/3 the amount of field measurements that a three-axis, fixed magnetometer provides in a static test facility. The research described in this document has two objectives: To estimate the magnetic signature of a small surface vessel using AUV-acquired magnetic field magnitude measurements, and to assess the feasibility of using AUV-acquired magnetic field vector component measurements in the Earth's inertial frame for magnetic signature estimation.

AUVs with distributed control systems and magnetometers have been developed at the University of Idaho (UI) for the purpose of applied research, including underwater electromagnetic sensing. Improvements in the calibration of the onboard magnetometers using a land calibration method reduced the noise floor in magnetic field measurements to less than 10 nT [8]. Inverse model magnetic signature estimation has been performed for a simple case–a small, fiberglass hull surface vessel with a bar magnetic attached to the bow–using least-squares and the magnitude of the measured magnetic field [9].

978-0-933957-40-4 ©2013 MTS

II. METHODS

A. AUVs and AUV Sensors

Measurements were taken with a fleet of AUVs, each equipped with a tri-axial, fluxgate magnetometer. The onboard control system consisted of five microcontrollers, connected by Ethernet [10]. Acoustic signals were used for fleet communications and fleet controls [11]. Onboard AUV processors handled position estimation, navigation, and attitude control using an extended Kalman filter (EKF) algorithm and a proportional-integral-derivative (PID) controller [11]. Details of the AUV system have been documented elsewhere [10] [6]. Features relevant to the work described in this paper are discussed here in detail.

The magnetometer voltage signals for each axis were sampled by an onboard digital signal processor (DSP) at a frequency of 16 kHz. Timing of the sampling process was directly regulated by a GPS pulse-per-second (PPS) signal. Measurements indicated that the PPS signal drift when underwater was on the order of ~200μs in one hour [12]. The magnetometer signals were processed and a calibration described in [6] was applied. The result of this procedure was magnetic flux density measurements $\vec{B} = [B_x \quad B_y \quad B_z]$ – herein called B-field measurements–in three orthogonal directions relative to the AUV frame.

Each AUV also contained a six degree of freedom (DOF) inertial measurement unit (IMU) and magnetic compass capable of three-dimensional orientation estimation measurements. The IMU sent measurement signals at 100 Hz over a serial connection to one of the microcontrollers on the AUV. These measurements were sampled from a buffer at 16 Hz and recorded. The magnetic compass also sent signals over a serial port at a sampling rate of 4 Hz. The microcontroller assigned timestamps to the IMU and compass measurements. These time-stamps were regulated by the same GPS PPS that regulated the sampling of magnetometer voltages.

B. Magnetic Signature Measurements

Magnetic signature measurements were collected at the Acoustic Research Detachment (ARD) of the Naval Surface Warfare Center (NAVSEA) in Lake Pend Oreille, Bayview, ID. Lake Pend Oreille is a deep fresh-water lake with low acoustic noise and minimal background magnetic fields. Five acoustic transponders, fixed to the lake bottom, were used for AUV navigation. Acoustic messages from the transponders were used to regulate formation behavior. An independent acoustic tracking system with an accuracy of 0.01-0.6 m [13] was used for measurement of AUV location during experiments.

Post-processing was used to estimate AUV position for the B-field measurements. A post-processing EKF algorithm and a non-causal Rauch-Tung-Striebel (RTS) smoothing algorithm were used to ameliorate the estimated AUV position, recorded onboard while the measurements were taken according to methods described in [6]. These positions were then matched according to timestamps with the B-field measurements.

A 2.24 m wide, 8.23 m long surface vessel, constructed with a fiberglass hull and outfitted with a differential global positioning system (dGPS), was used as a test subject for magnetic signature measurements. The fiberglass hull gave the vessel a relatively small magnetic signature. Additional suspected sources of the intrinsic surface vessel magnetic signature were thought to be a generator, the motors, a propeller guard, and a fuel gauge near the center of the vessel. A sketch of the surface vessel showing these components is shown in Fig. 1. In this figure, and in subsequent discussion, the coordinate frame XYZ is used to indicate position relative to the surface vessel. The orientation of the Z direction is up.

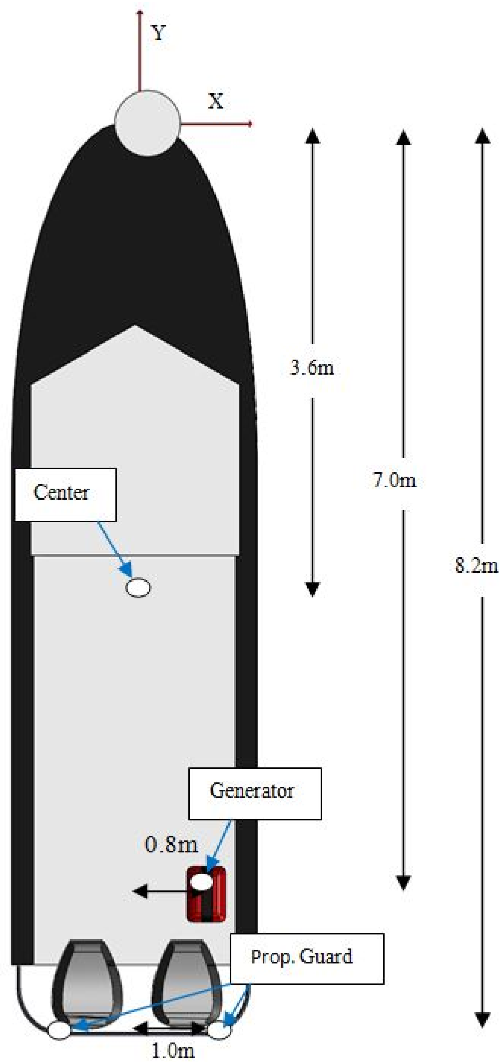

Fig. 1. Magnetic dipole locations (white ovals) on the surface vessel for intrinsic magnetic signature estimation.

For some of the experiments, the surface vessel was equipped with a permanent bar magnet below the bow, ~0.3 m from the water surface. The bar magnet had a reported dipole moment of 135 Am^2 and was mounted to the surface vessel so that the dipole moment vector was $\vec{m} = [m_x \quad m_y \quad m_z] = [0 \quad 0 \quad 135]$ Am^2 in the XYZ coordinate frame. The experiments conducted while the bar magnet was attached are herein called bar magnet surface vessel passes. The experiments conducted without the bar magnet attached are herein called intrinsic magnetic surface vessel passes.

The magnetic signature measurements were performed by passing an AUV formation at nominal depths ranging from 3-

7m underneath the moving surface vessel. The AUV formation and the surface vessel proceeded in opposite directions along a straight line during the pass. The speed of the AUV formation and the surface vessel were ~0.7 m/s and ~1.5 m/s respectively.

C. Magnetic Signature Modeling Using AUV-Acquired Measurements

AUV-acquired magnetic signature measurements were used to determine a magnetic model of the surface vessel. B-field magnitude $|B|$ was computed from measurements of B_x, B_y, and B_z in the AUV frame. The signature model was assumed to consist of magnetic dipoles located at positions of components that were suspected of contributing to magnetic signature. A least-squares procedure was used to estimate dipole moments that produced a model that best matched the AUV-acquired measurements.

D. Determination of Magnetic Signature Vector Components

Since the AUVs were equipped with a tri-axial magnetometer measuring B-field components B_x, B_y, and B_z, it was in principle possible to determine the components $\overline{B_x}$, $\overline{B_y}$, and $\overline{B_z}$ of the magnetic signature of the surface vessel. To enable this, it is necessary to transform the B-field components B_x, B_y, and B_z in the AUV frame to the frame XYZ of the surface vessel. Axis directions for both frames are shown in Fig. 2. In subsequent discussions, it is assumed that the surface vessel frame is identical to the inertial frame.

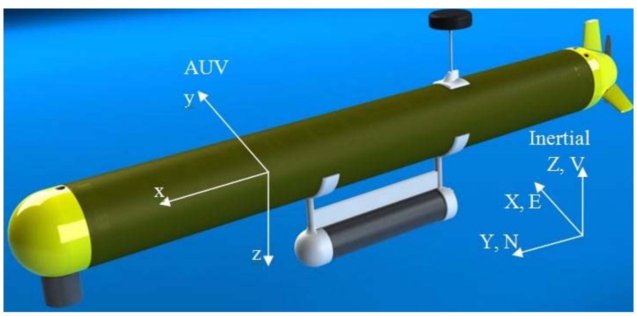

Fig. 2. Axis directions for the AUV and the inertial reference frames. In the inertial frame, East direction coincides with X direction, North direction coincides with Y direction, and vertical up direction coincides with Z direction.

The reference frame transformation can be realized by a 3-dimensional Euler angle rotation matrix. The inverse of the commonly used aerospace sequence rotation matrix R_I is [14]

$$R_I{}^{-1} = \begin{bmatrix} c\theta c\psi & s\varphi s\theta c\psi - c\varphi s\psi & s\varphi s\psi + c\varphi s\theta c\psi \\ c\theta s\psi & c\varphi c\psi + s\varphi s\theta s\psi & c\varphi s\theta s\psi - s\varphi c\psi \\ -s\theta & s\varphi c\theta & c\varphi c\theta \end{bmatrix}, \quad (1)$$

where, c and s are the cosine and sine functions, and φ, θ, and ψ are the Euler angles roll, pitch and heading, respectively. The 3-dimensional rotation matrix transformed components into an inertial reference frame $[North \quad East \quad Down]$ [14]. To separate the background magnetic field from the magnetic signature of the surface vessel, predicted values of the Earth's magnetic field from the World Magnetic Model (WMM) [15] were used. The predicted values for the Earth's magnetic field from the WMM are given in a coordinate system $[East \quad North \quad Up]$. To transform B-field components into this coordinate system, the rotation matrix

$$R_E = \begin{bmatrix} 0 & 1 & 0 \\ 1 & 0 & 0 \\ 0 & 0 & -1 \end{bmatrix} \quad (2)$$

was required. The transformation of AUV-acquired B-field components B_x, B_y, and B_z into surface vessel coordinate system components $\overline{B_x}$, $\overline{B_y}$, and $\overline{B_z}$ was

$$\begin{bmatrix} \overline{B_x} \\ \overline{B_y} \\ \overline{B_z} \end{bmatrix} = R_E R_I{}^{-1} \begin{bmatrix} B_x \\ B_y \\ B_z \end{bmatrix}. \quad (3)$$

AUV-acquired measurements of roll φ, pitch θ and heading ψ from the IMU and compass were necessary for the transformation. Something noteworthy in the transformation was that the $\overline{B_z}$ component did not depend on the AUV heading ψ.

E. Experimental Uncertainty Propagated to Magnetic Signature Vector Components

To determine the propagation of uncertainty into the surface vessel magnetic signature components $\overline{B_x}$, $\overline{B_y}$, $\overline{B_z}$ from the magnetometer measurements and the orientation measurements, laboratory experiments were conducted. AUV measurements of roll φ, pitch θ and heading ψ were recorded while the AUV was statically positioned approximately planar to the Earth's surface. The root-mean-square (RMS) variation in roll σ_φ, pitch σ_θ, and heading σ_ψ were computed. The AUV motor was turned on during the experiment to emulate vibration effects likely encountered during surface vessel pass experiments.

Measurements of roll φ and pitch θ from two sensor sources on the AUV were considered during the experiments. The compass directly provided measurements of roll φ, pitch θ and heading ψ. Roll φ_{IMU} and pitch θ_{IMU} were also calculated from IMU accelerometer measurements of acceleration, a_x, a_y, a_z using [16]

$$\theta_{IMU} = -sin^{-1}(a_x), \quad (4)$$

$$\varphi_{IMU} = tan^{-1}\left(\frac{a_y}{a_z}\right). \quad (5)$$

In this formulation, measured AUV body accelerations were assumed negligible.

A root-sum-square analysis [17] was used to estimate the propagation of RMS variation in AUV acquired measurements of B-field components σ_{B_x}, σ_{B_y}, and σ_{B_z} and roll σ_φ, pitch σ_θ, and heading σ_ψ to RMS variation in magnetic signature components $\sigma_{\bar{B}_x}$, $\sigma_{\bar{B}_y}$, and $\sigma_{\bar{B}_z}$. The transformation model (3) was used in the analysis.

III. Experimental Results and Discussion

A. Magnetic Signature Modeling Using Measurements of Magnetic Field Magnitude

Two magnetic signature models were considered to explain the B-field magnitude $|B|$ measurements, independent of coordinate reference frames, by a formation of three AUVs. A comparison of the measurements and models are shown in Figs. 3 and 4.

In Fig. 3, a magnetic signature model consisting of a single dipole located at the position of a small-motor generator at $[X \quad Y \quad Z] = [0.8 \quad -7.0 \quad 0.4]$ m is shown. Least-squares was used to determine a dipole moment of $\vec{m} = [m_x \quad m_y \quad m_z] = [7.2 \quad 21.5 \quad -32.1]$ Am^2 at this location. In Fig. 3a, the measurements of B-field magnitude |B| at horizontal positions relative to the surface vessel are coded by color. The measurements shown are aggregated from three passes of the formation of AUVs under the surface vessel. The measurements indicated that the magnetic signature of the surface vessel was ~100nT in magnitude. The spatial distribution was roughly circularly symmetric, with the exception that higher levels of ~100nT extended to the starboard side at the stern. The extent of the signature spanned a diameter of ~10 m. Higher B-field values consistently occurred directly underneath the surface vessel, and reduced more-or-less monotonically with horizontal distance from the vessel. Small departures from the monotonic nature of the signature were observed. Some of these departures may be explained by the fact that depths of individual AUVs were staggered by 0.5m relative to the nominal formation depth of 3.5m.

In Fig. 3b, the magnitude of the magnetic signature model from the single dipole model of $\vec{m} = [m_x \quad m_y \quad m_z] = [7.2 \quad 21.5 \quad -32.1]$ Am^2 located at $[X \quad Y \quad Z] = [0.8 \quad -7.0 \quad 0.4]$ m is plotted versus position relative to the surface vessel at the nominal AUV formation depth of 3.5m. Upon comparison with the signature measurements in Fig. 3a, it appears that the model is a reasonable representation.

In Fig. 3c, residuals between the single dipole model $\vec{m} = [m_x \quad m_y \quad m_z] = [7.2 \quad 21.5 \quad -32.1]$ Am^2 located at $[X \quad Y \quad Z] = [0.8 \quad -7.0 \quad 0.4]$ m and measurements shown in Fig. 3a are plotted versus position relative to the surface vessel. In the computation of residuals, the difference between B-field magnitude $|B|$ predicted by the model at the staggered depths of individual AUVs and measured B-field magnitude $|B|$ was used. The residuals are relatively large in localized regions. For example, near $[X \quad Y \quad Z] = [0 \quad -2 \quad 3.5]$ m, the residuals reach ~40 nT. Patterns in the residuals indicate that the single dipole model for the signature of the surface vessel may be insufficient, depending upon the required accuracy of the estimation.

An alternative magnetic signature model, consisting of four dipoles was then considered. The four dipoles were located at positions on the surface vessel shown in Fig. 1. These locations are also specified in columns 2-4 of Table I. A least-squares procedure was used to estimate dipole moments that predicted a magnetic signature best matching the AUV-acquired B-field magnitude $|B|$ measurements. The dipole moments determined by the least squares procedure at each location are shown in columns 5-8 of Table I.

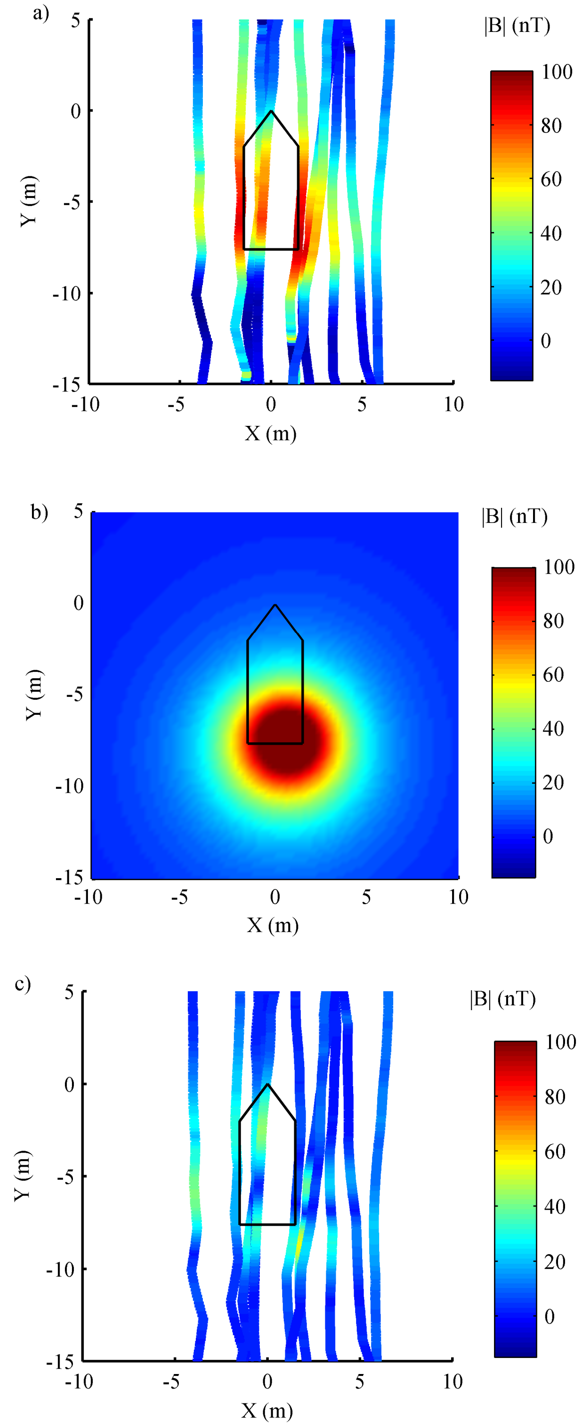

Fig. 3. a) Overhead view of measured B-field magnitude deviation from background field b) Field deviations spatially predicted from dipole moment at generator location c) Residuals from measured and predicted B-field magnitude deviation.

TABLE I. DIPOLE POSITIONS AND DIPOLE MOMENTS DETERMINED BY LEAST-SQUARES

Dipole Discription	Dipole Location (m)			Estimated Dipole Strength (Am^2)			
	X	Y	Z	m_x	m_y	m_z	$\|m\|$
Generator	0.8	-7.0	0.4	2.9	61.8	-19.2	64.8
Prop Guard	1.0	-8.2	0.4	-16.8	12.8	-4.1	20.9
Prop Guard	-1.0	-8.2	0.4	21.4	-29.3	-23.6	43.3
Center	0.0	-3.8	0.4	-11.2	9.3	-8.6	16.9

In Fig. 4, the magnetic signature from the 4-dipole model and the residuals between the 4-dipole model magnetic signature and AUV-acquired magnetic signature measurements are shown. In Fig. 4a, the predicted B-field magnitude $|B_p|$ versus position relative to the surface vessel at the nominal depth (3.5m) of the AUV formation is shown. In Fig. 4b, the residuals versus position relative to the surface vessel are shown. It is appears that the model signature shown in Fig. 4a is a better qualitative representation of the measured signature, shown in Fig. 3a, in that it is not entirely circularly symmetric. In addition, the residuals shown in Fig. 4b are less than 20nT, and do not contain large isolated peaks to the degree observed in residuals using the single dipole model.

A temporal presentation of AUV-acquired B-field magnitude $|B|$ measurements and predicted B-field magnitude $|B_p|$ using the 4-dipole model is shown in Fig. 5. In Fig. 5, a concatenation of individual temporal segments of each AUV pass near the surface vessel is shown. AUV and surface vessel positions during the same sample times as the measurements were used to predict B-field magnitude $|B_p|$ from the 4-dipole model.

Of the eleven individual passes shown in Fig. 5, ten show close agreement between measured $|B|$ and predicted B-field magnitude $|B_p|$. The measurements show a peak in B-field magnitude $|B|$ of ~35-90 nT. The peak value depended on the distance of the nearest pass by each AUV. The peak values of ten of the individual AUV measurements were within 5nT of the predicted values. One set of the AUV-acquired measurements did not closely match the predicted signature. This was attributed to a poor navigation fix on AUV position during that pass.

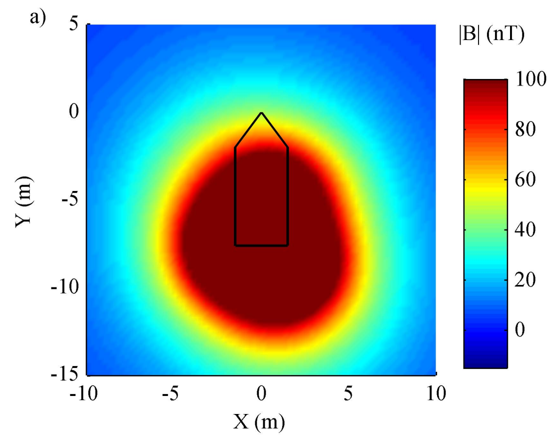

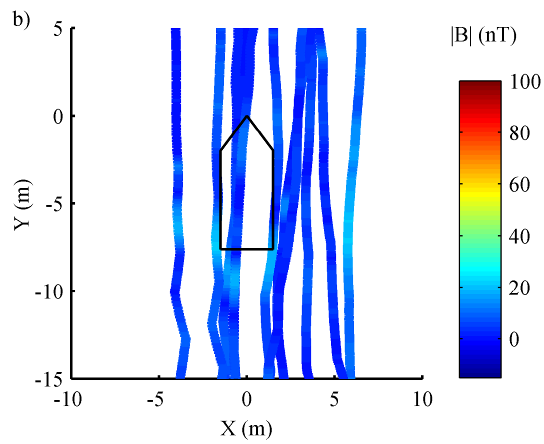

Fig. 4. a) Overhead view of B-field magnitude deviations spatially predicted from using the 4-dipole model. c) Residuals from measured and predicted B-field magnitude deviation using the 4-dipole model.

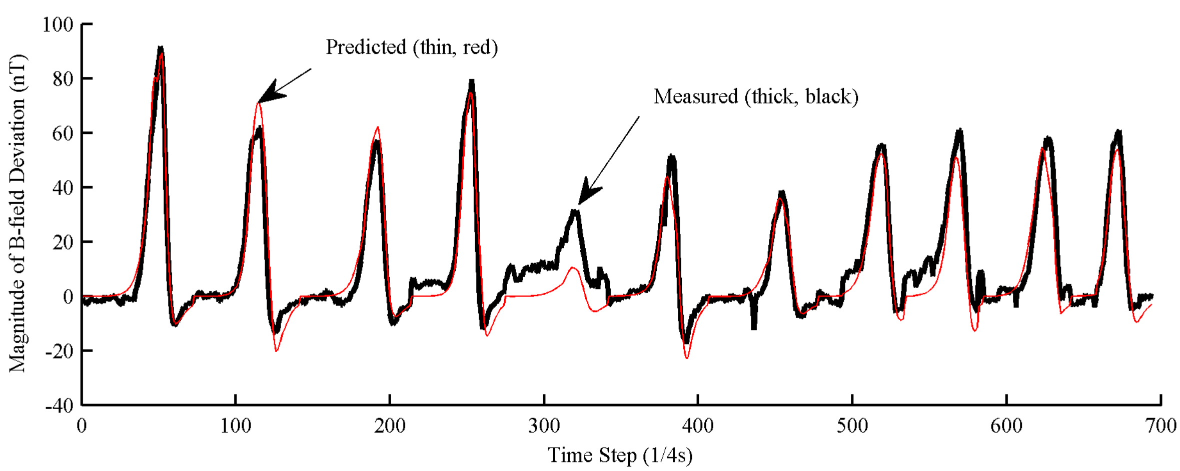

Fig. 5. Concatenated measured and predicted deviations from the four dipole moment estimation using measurements from an intrinsic surface vessel pass.

TABLE II. PREDICTED AND OBSERVED RMS NOISE IN MAGNETIC VECTOR COMPONENTS FROM ORIENTATION ESTIMATION BASED ON COMPASS AND IMU MEASUREMENTS FROM THE UNCERTAINTY PROPAGATION ANALYSIS AND DURING A LABORATORY EXPERIMENT.

Angle Source	Input Mean		Input RMS		Predicted RMS from Uncertainty Propagation Analysis[a]			Actual RMS Observed from Laboratory Experiment[a]		
	Roll, Pitch, Heading (deg.)	Bx, By, Bz (nT)	Roll, Pitch, Heading (deg.)	Bx, By, Bz (nT)	Bx (nT)	By (nT)	Bz (nT)	Bx (nT)	By (nT)	Bz (nT)
Compass	3.2907, -2.4805, 2.2450	11477, 26761, -46408	0.0097, 0.0350, 0.0479	35.85, 25.79, 11.19	43.5	39.6	21.0	41.0	38.8	20.9
IMU a_x, a_y, a_z/ Compass ψ	0.4861, 1.5460, 2.2448	11477, 26761, -46408	0.0255, 0.0290, 0.0479	35.85, 25.79, 11.19	46.3	36.7	17.9	50.6	35.3	17.4

a. B-field vector components in columns 6-11 are in the inertial frame

B. Measurement of Magnetic Field Signature Components

As described previously, measurement of magnetic signature components relative to the inertial frame requires simultaneous measurement of AUV orientation for the transformation of AUV-acquired magnetometer measurements to the inertial frame.

A baseline analysis of expected uncertainty in measurement of magnetic signature components is contained in Table II. The observed indicated mean of roll φ, pitch θ and heading ψ and magnetic field components B_x, B_y and B_z in the AUV frame are contained in the first two columns. Roll φ, pitch θ and heading ψ measured exclusively from the compass is shown in the first row, while roll φ and pitch θ from the IMU accelerometers and heading ψ from the compass is shown in the second row. The observed RMS variation in roll σ_φ, pitch σ_θ, heading σ_ψ, and in the components σ_{B_x}, σ_{B_y}, and σ_{B_z} in the AUV frame are shown in the fourth and fifth columns. The expected uncertainty in components $\overline{B_x}$, $\overline{B_y}$ and $\overline{B_z}$ in the inertial frame based on the propagation of uncertainty model is contained in the sixth through eighth columns of Table II. As a check, the measurements of B-field components B_x, B_y and B_z were transformed using the acquired orientation measurements to obtain the B-field components $\overline{B_x}$, $\overline{B_y}$ and $\overline{B_z}$ in the inertial frame, and the associated RMS variation was computed. These results are contained in the ninth through eleventh columns of Table II.

Results from a representative laboratory experiment, contained in Table II, help quantify the capability of the particular AUVs being used for measurement of magnetic signature to determine B-field components in the inertial frame. RMS variation in B-field components ranging from ~18-46nT can be expected. RMS variation in $\overline{B_x}$ and $\overline{B_y}$ ranged from ~37-46nT, somewhat higher than that of $\overline{B_z}$, which ranged from ~18-21nT. This was attributed to the fact that the transformation computation for $\overline{B_z}$ did not contain a contribution from RMS variation in heading σ_ψ.

The AUV orientation roll φ and pitch θ, derived from measurements of IMU accelerations a_x, a_y, a_z, and heading ψ obtained from the compass, were used to compute magnetic signature components $\overline{B_x}$, $\overline{B_y}$ and $\overline{B_z}$ in the inertial frame from AUV measurements of B_x, B_y and B_z in the AUV frame. AUV bar magnet surface vessel passes were used. According to Table II, RMS variation in $\overline{B_z}$ of ~17nT would

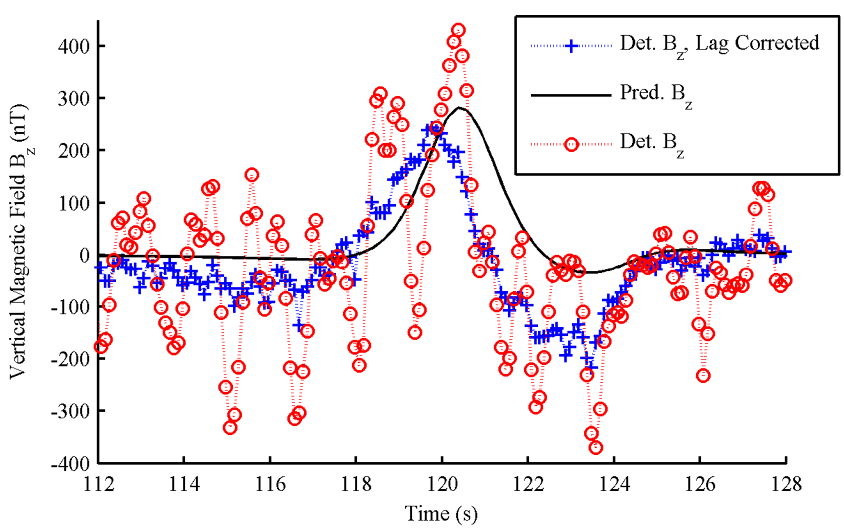

Fig. 6. Comparison of the vertical magnetic field vector component after transformation from a surface vessel pass using roll and pitch calculated from IMU accelerometer measurements.

be expected. In Fig. 6, the vertical component $\overline{B_z}$ for a temporal segment of an individual pass underneath the surface vessel is shown (open circles), along with the predicted field of the magnet (solid line) using the reported bar magnet dipole moment of 135 Am^2. A third measurement (pluses) is also shown on Fig. 6, which will be explained subsequently.

From Fig. 6, it is apparent that the predicted z component of the magnet mounted to the surface vessel was ~300nT in magnitude. The AUV-acquired measurement, using IMU accelerations and compass heading resembled the prediction, but suffered from noise well in excess of ~18 nT expected from the uncertainty analysis.

Effort was given to determine the cause of excess noise in the AUV-acquired measurement of surface vessel magnetic signature component $\overline{B_z}$. Visual inspection of acquired data revealed a time-lag between IMU acceleration measurements a_x, a_y, a_z and magnetometer voltage measurements that became the B-field components B_x, B_y and B_z.

To support visual observation of the time-lag, a cross-correlation analysis between magnetometer measured voltage and IMU measured acceleration was conducted. A cross correlation between magnetometer measured voltage V_x and IMU measured a_y (x and y denoting the AUV frame axes) is shown in Fig. 7 over time-lags extending over an AUV pass. A peak cross-correlation was found at a time lag of -200 ms. This meant that the IMU measurements lagged the magnetometer measurements. The lag of ~200 ms was attributed to network latency in the acquisition of IMU measurements.

When the IMU measurements of acceleration a_x, a_y, a_z were manually shifted in accordance with the lag indicated by the cross-correlation analysis, the AUV-acquired measurement

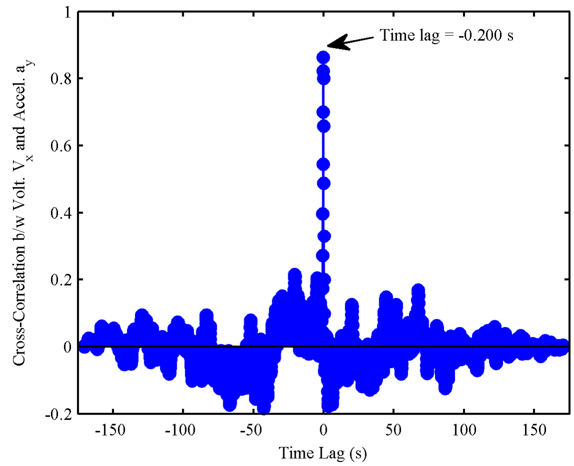

Fig. 7. Normalized cross-correlation between voltage measured by the magnetometer in the x-direction and acceleration measured by the IMU in the y-direction of the AUV frame. Time lags of -170 to 170 s (length of the experiment) were used for the analysis.

of magnetic signature component $\overline{B_z}$ drastically improved. In Fig. 6, the magnetic signature component $\overline{B_z}$ after correction of the time lag is shown annotated with pluses. The same segment of an AUV pass underneath the surface vessel as was used for the other data in the figure was used. It is apparent that the noise level in the component $\overline{B_z}$ was drastically improved, and in fact, appears to agree with the value of ~18 nT obtained from the uncertainty analysis.

A view of the magnetic signature components $\overline{B_x}$, $\overline{B_y}$ and $\overline{B_z}$ in the inertial frame obtained from an entire AUV bar

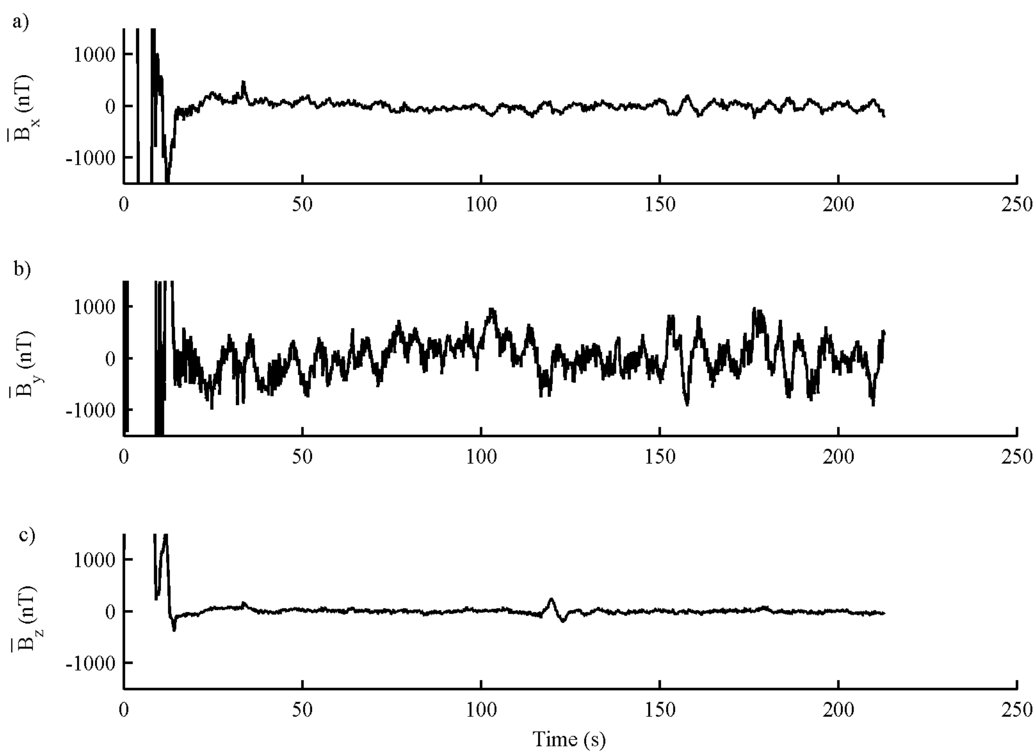

Fig. 8. Transformed magnetic vector components vs. time using the IMU acceleration measurements to estimate roll and pitch and the compass measurements to estimate heading during a bar magnet surface vessel pass.

magnet surface vessel pass is shown in Fig. 8. The same surface vessel pass used for Figs. 6 and 7 is used for Fig. 8. In Fig. 8a,b,c, the magnetic signature components $\overline{B_x}$, $\overline{B_y}$ and $\overline{B_z}$ components are plotted over a time duration of ~220 s. In Fig. 8c, the signature in the component $\overline{B_z}$, as observed in detail in Fig. 6, is clearly visible. The components $\overline{B_x}$, $\overline{B_y}$ appear to have very large variation, in excess of the 30-50nT predicted by uncertainty analysis summarized in Table II. However, the majority of the variation observed in $\overline{B_x}$, $\overline{B_y}$ was determined to be caused by heading estimation coming from compass measurements.

IV. Conclusions

Using magnetic field measurements acquired by AUVs, we were able to effectively estimate the magnetic signature of a surface vessel with a 4 dipole model. This was done without any prerequisite knowledge of the magnetic sources onboard the surface vessel. We also demonstrated the capability of determining the vertical magnetic field vector component B_z from magnetic field measurements and orientation measurements acquired by AUVs. This was accomplished with conventional sensor technology: an IMU, magnetic compass, and a fluxgate magnetometer all mounted to each AUV. A time delay between the IMU and magnetometer measurements of 200 ms was discovered and corrected. This demonstrated the impact of network latency on the magnetic field vector component determination in the inertial frame. The vertical magnetic signature component $\overline{B_z}$, determined from measurements, contained RMS noise observed to be near the predicted RMS noise of ~18 nT. This is 8.2% of the maximum value in the signature of ~220 nT.

V. Acknowledgements

The authors are grateful for the support of the Office of Naval Research through the grant *Electromagnetic Signature Assessment System Using Multiple Autonomous Underwater Vehicles (AUVs)* Phase III, ONR N00014-10-1-0883, the assistance of Doug Odell, Thomas Bean and other personnel at the NSWC Carderock Acoustic Research Detachment, and the assistance of Bryce Gill and Ryan Borth at the University of Idaho.

References

[1] J. J. Holmes, *Exploitation of Ship's Magnetic Field Signatures*. San Francisco: Morgan & Claypool Publishers, 2006.

[2] G. Jeung, C. Yang, H. Chung, S. Lee, D. Kim, "Magnetic Dipole Modeling Combined with Material Sensitivity Analysis for Solving an Inverse Problem of Thin Ferromagnetic Sheet," *IEEE Transactions on Magnetics*, vol. 45, no. 10, pp. 4169-4172, October 2009.

[3] J. J. Holmes, *Modeling a Ship's Ferromagnetic Signatures*. San Francisco: Morgan & Claypool Publishers, 2007.

[4] J. Coulomb, G. Cauffet, J. Bongiraud O. Chadebec, "How to Well Pose a Magnetization Identification Problem," *IEEE Transactions on Magnetics*, vol. 39, no. 3, pp. 1634-1637, May 2003.

[5] J. B. Nelson and J. C. Richards, "Magnetic Source Parameters of MR OFFSHORE Measured during Trial MONGOOSE 07," Defense R&D Canada-Atlantic, Technical Memorandum 2007.

[6] C. R. Walker, J. Q. Stringfield, E. T. Wolbrecht, M. J. Anderson, J. R. Canning, Thomas A. Bean, Douglas L. Odell, James. F. Frenzel, Dean B. Edwards, "Measurement of the Magnetic Signature of a Moving Surface Vessel with Multiple Magnetometer-Equipped AUVs", Ocean Engineering, Vol. 64, pp. 80-87, 2013.

[7] M. Wynn and J. Bono, "Magnetic Sensor Operation On Board an AUV: Magnetic Noise Issues and a Linear Systems Approach to Mitigation," in *OCEANS '02 MTS/IEEE*, 2002, pp. 985-993.

[8] C. Walker et al., "Calibration and Localization of AUV-acquired Magnetic Survey Data," in *IEEE Oceans*, Kona, 2011, pp. 1-6.

[9] C. Walker et al., "Survey of the Magnetic Signature of a Moving Surface Vessel by Multiple AUVs," in *Oceans, 2012*, Hapton Road, 2012, pp. 1-7.

[10] G. J. Beidler and R. W. Wall, "Low Cost Distributed Control System for Autonomous Vehicles," in *OCEANS 2006-Asia Pacific*, 2006, pp. 1-7.

[11] G. Beidler, J. Canning, D. Odell, R. Wall, M. O'Rourke, M. Anderson, D. Edwards T. Bean, "Language and Logic to Enable Collaborative Behavior among Multiple Autonomous Underwater Vehicles," *Internation Journal of Intelligent Control and Systems*, vol. 13, no. 1, pp. 67-80, March 2008.

[12] B. Crosbie, M. Andersonl, E. Wolbrecht, J. Canning, and D. Edwards, "Synchronous Navigation of AUVs Using WHOI Micro-Modem 13-bit Communications," in *Proceedings of Oceans '10*, Seattle, 2010.

[13] Doug Odell, Jesse Pentzer, John Canning, and Dean Edwards, "A Versatile Tracking System for AUV Testing," in *IEEE Oceans*, Sydney, 2010.

[14] M. Cook, *Flight Dynamics Principles*. New York, NY: Wiley, 1997.

[15] NGA, NGDC, BGS. (2009, December) World Magnetic Model WMM2010.

[16] C. Jagadish and C. Chang, "Diversified Redundancy in the Measurement of Euler Angles Using Accelerometers and Magnetometers," in *Proceedings of the 46th IEEE Conference on Decision and Control*, New Orleans, LA, 2007, pp. 2669-2674.

[17] A. J. Wheeler and A. R. Ganji, *Introduction to Engineering Experimentation*, 2nd ed. Upper Saddle River, New Jersey: Pearson Education, Inc., 2004.